Int. J. Heat Mass Transfer. Vol. 28, No. 8, pp. 1415–1423, 1985
Printed in Great Britain

0017–9310/85 $3.00 + 0.00

Liquid–solid contact measurements using a surface thermocouple temperature probe in atmospheric pool boiling water*

L. Y. W. LEE and J. C. CHEN
Institute of Thermo-Fluid Engineering and Science, Lehigh University, Bethlehem, PA 18015, U.S.A.

and

R. A. NELSON†
MS-K553, Los Alamos National Laboratory, Los Alamos, NM 87545, U.S.A.

(*Received* 31 *October* 1983 *and in final form* 25 *September* 1984)

Abstract—The objective of this investigation was to apply the technique of using a microthermocouple flush-mounted at the boiling surface for the measurement of the local surface-temperature history in film and transition boiling on high temperature surfaces. From this measurement direct liquid–solid contact in film and transition boiling regimes was observed. In pool boiling of saturated, distilled, deionized water on an aluminum-coated copper surface, the time-averaged, local liquid-contact fraction increased with decreasing surface superheat. Average contact duration increased monotonically with decreasing surface superheat, while frequency of liquid contact reached a maximum of ~50 contacts s^{-1} at a surface superheat of ~100 K and decreased gradually to 30 contacts s^{-1} near the critical heat flux. The liquid–solid contact duration distribution was dominated by short contacts <4 ms for high surface superheats and shifted to long contacts >4 ms at low surface superheats, passing through a relatively flat contact duration distribution at about 80 K. The results of this paper indicate that liquid–solid contacts may be the dominant mechanism for energy transfer in the transition boiling process.

INTRODUCTION

MODELING of the post-critical heat-flux (post-CHF) regimes is important to light water nuclear reactor safety, as well as to other industrial applications where high temperature boiling surfaces may be encountered. Recent reviews by Winterton [1], and Groeneveld and Snock [2, 3] show that the transition and low temperature film boiling (near the minimum heat flux) regimes are not yet well understood.

In general, the modeling approach for these post-CHF regimes, originally suggested by Rohsenow [4], uses the concept that at any given instant, the boiling surface has liquid contacting part of the solid's surface, while vapor contacts the remainder, given by

$$q_{\substack{\text{total}\\ \text{post-CHF}}} = q_l F_A + q_v(1 - F_A). \quad (1)$$

Generally, liquid has much better thermal transport properties than its associated vapor, so that heat flux to the contacting liquid, q_l (by transient conduction, convection, and evaporation), is believed to be significantly greater than the heat flux to the vapor, q_v (by transient conduction and convection). The mechanisms that control the liquid–solid contact, and therefore the instantaneous liquid contact-area fraction, F_A, remain unclear in pool boiling [1, 5], as well as in forced flow situations [1].

An alternate approach assumes that the process being represented is ergodic, so that instead of working in terms of an instantaneous, liquid contact-area fraction, the total post-CHF heat flux can be written as

$$q_{\substack{\text{total}\\ \text{post-CHF}}} = q_l F_\theta + q_v(1 - F_\theta) \quad (2)$$

in terms of a local liquid contact-time fraction, F_θ.

If the area over which a boiling experiment is performed is of sufficient size that a statistically sufficient number of the controlling phenomena (such as Taylor waves) are included in the area average, a valid F_A can be obtained. Similarly, if the time over which the same phenomena occur is sampled for a sufficiently long time to include a statistically sufficient number of occurrences at a point on the surface, a valid measurement of F_θ can be obtained. If these criteria are met, then the assumption of an ergodic process implies that

$$F_A = F_\theta. \quad (3)$$

It is important to note that the determination of F_θ also implies some minimum size requirement. This is implicit within the term 'same phenomena' used above. For example, if the Taylor wave mechanism controls the phenomena, the boiling surface must be of sufficient size to allow several wavelengths, but does not have to be large enough to obtain a statistically valid F_A.

Studies of the transition and low temperature film boiling regimes in pool boiling have progressively

* Work supported by the U.S. Nuclear Regulatory Commission, Office of Nuclear Regulatory Research, under DOE Contract No. DE-AC07-761D01570.

† Work done while this author was at LOFT Program Division, EG&G Idaho, Inc., P.O. Box 1625, Idaho Falls, ID 83415, U.S.A.

NOMENCLATURE

c	specific heat [J kg^{-1} K^{-1}]
F_A	instantaneous liquid contact-area fraction [dimensionless]
F_θ	local liquid contact-time fraction [dimensionless]
F_{SA}	instantaneous liquid contact 'small area' fraction [dimensionless]
g_0	gravitational constant
k	thermal conductivity [W m^{-1} K^{-1}]
N	number of liquid–solid contacts in sample window
q	heat flux [W m^{-2}]
T	temperature [K].

Greek symbols

α	thermal diffusivity [m^2 h^{-1}]
ΔT_{sat}	surface superheat, $T_w - T_{sat}$ [K]
θ	time [s]
$\lambda_{1d,2d}$	one-dimensional and two-dimensional wave-lengths, respectively [m]
ρ	density [kg m^{-3}]
σ	surface tension [N m^{-1}].

Subscripts

A, B, C	time regions denoted in Fig. 4
c	contact
f	saturated liquid
g	saturated vapor
i	initial state
j	summation index
l	liquid
sat	saturation
total	total of quantity subscripted
v	vapor
w	wall or surface.

shown the potential influence of liquid–solid contacts. Originally, Westwater and Santangelo [6] and Stock [7] made high-speed motion pictures of boiling and concluded that there was no liquid–solid contact in these regimes. Berenson's study [8] later provided indirect evidence that liquid–solid contact did occur, because the boiling curve was affected by a change in solid materials and surface conditions. Bradfield [9] performed electric conductance measurements and confirmed that liquid–solid contacts actually did occur in the post-CHF regimes and that such contacts extended well into the film boiling regime.

One of the early models utilizing the concept represented by equation (1) was that proposed by Bankoff and Mehra [10]. They assumed that the majority of the heat transferred came from the liquid term and employed only the transient conduction phenomenon as the principal component to represent the liquid–solid contacts. While they did not directly calculate F_A, they did estimate average contact times. Numerous other authors have followed similar procedures of assuming various forms of q_l and q_v in order to infer F_A.

In an effort to measure the F_A for pool boiling, Yao and Henry [11, 12] used an electrical conductance probe over the entire boiling area and studied contact phenomena in stable film boiling of ethanol and water. They reported the frequency of contact, duration of contact, and F_A. However, due to the inherent uncertainties in the probe's calibration curve, reported liquid contact area fractions may be in error by factors of 2–5. Also, it is not clear that their boiling surface was of sufficient size to obtain a statistically valid F_A. A valid F_A measurement of a steady-state experiment should yield no frequency and duration information, yet this is reported in the paper.

In an effort to measure the F_θ of pool boiling water, Nishikawa *et al.* [13] used small (0.5-mm diameter) thermocouples embedded 4 mm beneath the boiling surface and 'planted' microthermocouples (0.05-mm diameter) that were soldered into the surface and extended out through the boiling fluid. They reported frequency of contact, duration of contact, and limited F_θ data for superheats of 60 K or less. However, their measurements were made on an 8-mm diameter copper boiling surface that was of insufficient size to allow a wave controlled phenomenon in the post-CHF regime.

The present authors recently developed a similar fast response microthermocouple technique to measure F_θ in pool boiling [14]. The thermocouple's measurement junction was constructed as part of the boiling surface, but the thermocouple leads exited through the surface wall material, rather than through the boiling fluid. Preliminary measurements of F_θ relative to the maximum measured surface temperature were obtained and showed an increasing F_θ as the surface temperature decreased.

The dual-mode heat-transfer concept expressed by equations (1) and (2) is also used in models for forced, convective-flow boiling. Iloeje [15] related the parametric effects of mass flux, quality, flow history, flow regimes, and surface effects to the liquid–droplet, heat-transfer behavior, including both liquid–solid contact and droplet evaporation in the thermal boundary layer. Their experimental data agreed in trend with their theoretical predictions. More recently, Chen *et al.* [16] utilized the concept to include liquid–droplet heat transfer in the film-boiling, dispersed-flow regime by separate transient conduction, nucleation, and thin film evaporation mechanisms in order to represent a droplet contacting the solid. As with pool boiling, numerous other authors have followed similar

procedures to calculate either F_A, F_θ, or the total surface heat flux.

In an effort to measure the F_θ in forced flow, Ragheb and Cheng [17] developed a flush-mounted, electrical conductance probe to detect liquid–solid contact on the inner surface of a thick tube. Transient quenching experiments in post-CHF convective flow were performed and a sample F_θ was reported. Unfortunately, their recording medium was too slow in response for measurement of individual liquid contacts. Only the time-averaged probe signal was available, and frequency and contact duration information was not obtained. Their F_θ was reported as F_A by using equation (3).

The objective of this investigation was to apply the technique developed in ref. [14] to evaluate liquid–solid contact in atmospheric pool boiling water. This paper discusses the experiment, analyzes the data, presents results obtained from the experiments, and draws conclusions from the results.

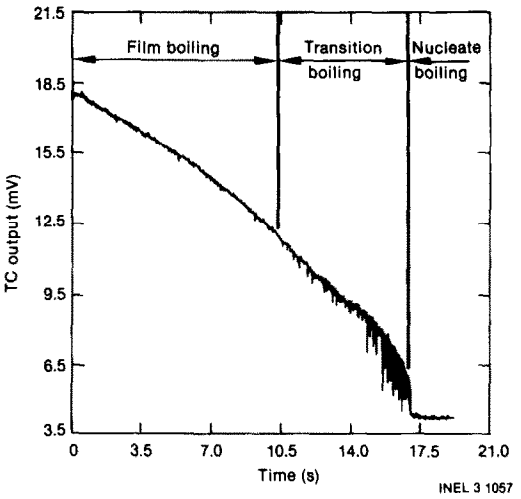

FIG. 2. Typical surface temperature history.

EXPERIMENTAL APPARATUS

Liquid–solid contact measurements were obtained during transient quenching experiments in the present experiment, using a fast-response surface microthermocouple. The thermocouple was constructed from a 0.51-mm (sheath diameter) microthermocouple inserted axially and silver-soldered into the center of a copper block as shown in Fig. 1. The thermocouple tip was initially extended above the block surface and was then cut flush with the block surface and polished flat. To bridge the open thermocouple leads and form a new thermocouple junction, a thin layer of aluminum was deposited on the entire surface top by vacuum vapor disposition. After six multiple coatings the probe surface had an estimated junction thickness of 0.016 mm and offered an optimum tradeoff between junction ruggedness and response time.

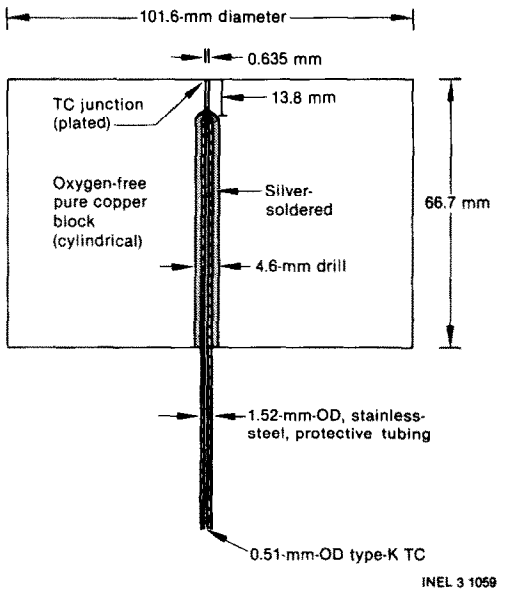

FIG. 1. Cross section of test block.

EXPERIMENTAL TECHNIQUE

To initiate an experiment, the test block-probe assembly shown in Fig. 1 was placed in a clam-shell oven and preheated to 720 K. After a uniform block temperature was obtained by holding the oven at temperature for 10 min, saturated deionized water was introduced onto the block-probe surface and contained by an aluminum skirt. A smooth transition from film boiling, to transition boiling, to nucleate boiling occurred as the block gradually cooled. A typical quench lasted 3–4 min. During the quench, water on the block was maintained at ~4 cm depth. Figure 2 shows a typical trace of the surface-probe response during the final phase of the quench process.

The temperature signal from the probe for a quench run was recorded and analyzed using the experimental setup shown in Fig. 3. The signal from the probe was amplified and recorded in real time with an FM recorder. A digital oscilloscope provided real time monitoring and also digitized the playback signal from the FM recorder at various sampling rates. The

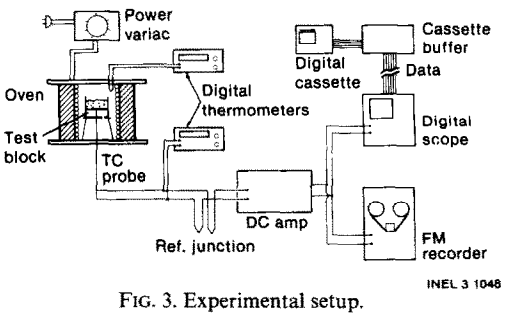

FIG. 3. Experimental setup.

digitized signal could then be transferred to a data cassette tape and later interfaced with the main frame computer for calculational purposes.

The measurements obtained from the micro-thermocouple probe provided two types of information regarding the boiling process during the quench history: the liquid–solid contact characteristics and the local surface temperature. These two types of results are presented and discussed below.

LIQUID–SOLID CONTACTS

Figure 4 shows a sample of the probe signal during a short window in the quench transient. When local film-boiling conditions (a vapor film levitating the liquid) exist over the probe surface, a high surface temperature is registered (Fig. 4, region A). As the vapor film is temporarily displaced from the hot wall, direct liquid–solid contact results, with transient conduction removing heat from the block surface. This removal rate is 2–3 orders of magnitude higher than that encountered when vapor covers the surface [14] and a sudden drop in surface temperature is observed (Fig. 4, Region B). Then, when the liquid is again expelled from the surface and dryout occurs, the surface temperature returns to a more elevated superheat (Fig. 4, Region C). Thus, the period of time that liquid contacts the block surface, θ_l, is that duration denoted by region B, θ_B. The F_θ for Fig. 4 would then be given by

$$F_\theta = \theta_B/(\theta_A+\theta_B+\theta_C). \tag{4}$$

Generalization of this procedure for an arbitrary sample window having N liquid–solid contacts yields the relationship

$$F_\theta = \sum_{j=1}^{N} \theta_{l,j}/\theta_{\text{total}}. \tag{5}$$

A further discussion of the criteria used to distinguish such liquid contacts from the probe signal and a discussion of the error associated with this time domain information are given in ref. [18].

It is widely accepted that at high surface superheats, a relatively stable vapor film exists between the hot surface and the bulk liquid. As the surface temperature

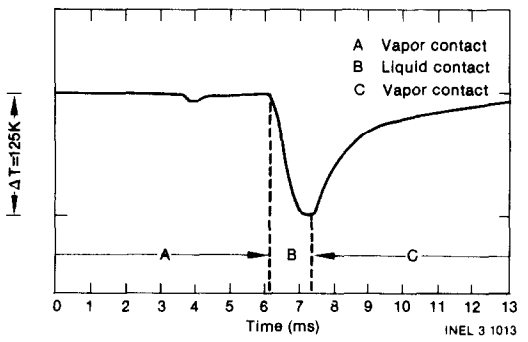

FIG. 4. Typical local surface temperature history for a liquid–solid contact.

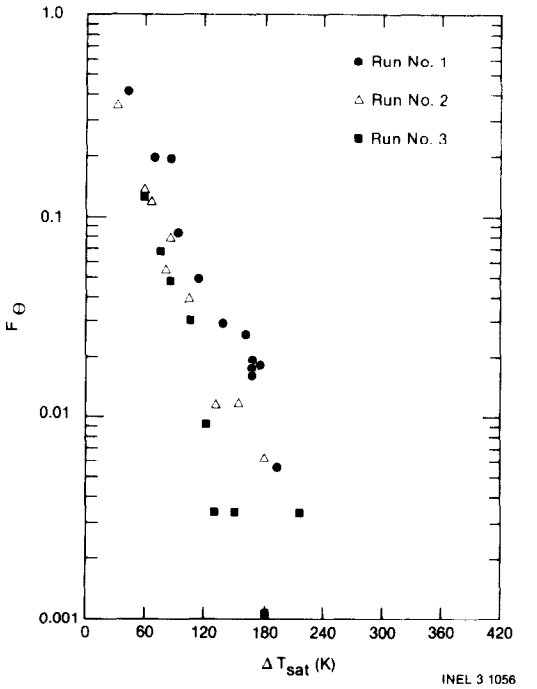

FIG. 5. Time-averaged liquid contact fraction as function of surface superheat.

gradually lowers, the vapor film becomes increasingly unstable and the surface area having liquid contacting it increases. A plot of the local liquid contact-time fraction is shown for three quench runs in Fig. 5 and supports this theory. The quantity plotted as the abscissa of Fig. 5 and other figures to follow is the surface superheat, ΔT_{sat}, determined by using the time-average of the probe-measured surface temperature. The local surface temperature will be discussed in detail in the next section.

From Fig. 5 several interesting factors can be noted (in addition to the dominant characteristic of decreasing F_θ) with respect to increasing surface superheat. The trends of the data indicate that $F_\theta \to 1.0$ somewhere between superheats of 0 K and about 30 K, as it should. Also, F_θ becomes very small for surface superheats >200 K. For superheats between 90 and 160 K, where the number of contacts are reasonable and the statistics have indicated a maximum error of about 10% (90% confidence), the scatter in the data is the greatest. This is interpreted as indicating a boiling regime subject to variations in the physical phenomena. It may, for example, reflect the aging of the boiling surface; however, this cannot be proven for the current experiment. At lower surface superheats (around 30–60 K), the variations within F_θ are within the maximum error of about 40% (90% confidence), and not order of magnitude variations as at the higher superheats. Whether this is a more stable boiling regime as supported by Lee's [19] heat flux analysis, or just an occurrence resulting from the statistics of the current study must be determined by further investigation.

A comparison of a typical F_θ (run 1) can be made to

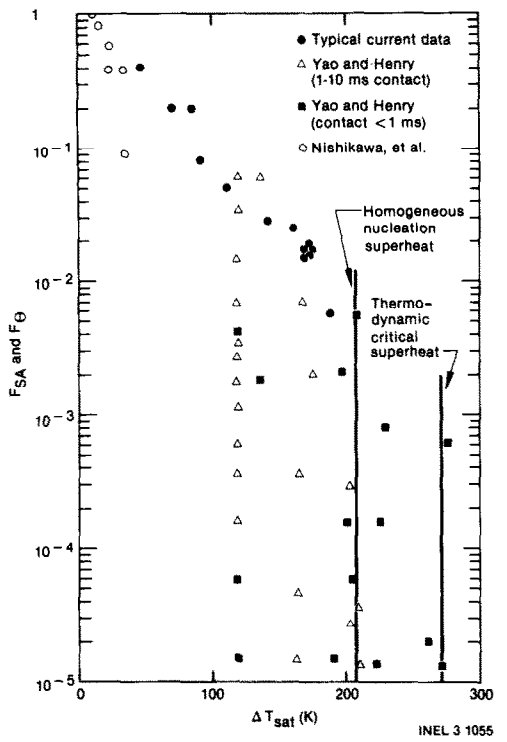

FIG. 6. Comparison of current typical results to those of Fig. 9 of ref. [11].

the results obtained by Yao and Henry [11, 12] for their F_A (see Fig. 6). Generally, F_θ from the current experiments lies close to the upper bounds of the F_A data. Considering the three major differences between the two experiments, the results are in surprisingly good agreement. First, the current experiment was run using an aluminum coating of the block's boiling surface and was done in air (so that surface oxidation would occur), as opposed to the Yao and Henry experiments, in which the copper block was gold plated and the experiment performed in an inert argon atmosphere (producing a non-oxidized surface). Second, the calibration uncertainty of the Yao and Henry probe involved factors of 2–5. Third, a potential difference between the two experiments arises from possible copper block size limitations, because the size of the Yao and Henry test block was not specified—only an indication that "liquid geometries with diameters greater than the fastest growing wave length were considered". As indicated in the introduction, in order for a valid area average measurement of F_A to be obtained, a large enough area must be considered in order that a statistically sufficient number of wavelengths exist over the boiling surface. It is not clear whether the Yao and Henry experiments meet this requirement, because (as shown in Fig. 6, which reproduces Fig. 9 of ref. [12]) contact duration information is given, implying that the size is not sufficient to obtain true instantaneous, area-averaged statistics. A true steady-state or pseudo-steady-state area-averaged liquid contact fraction measurement should not produce contact duration information.

Thus, it appears that the signal from the Yao and Henry probe should also be time-averaged, in order to obtain a liquid contact fraction against which to compare. Since the frequency of contact information is missing for each contact in ref. [12] and the interrelationship between each contact is missing in ref. [11], the integration with respect to time cannot be done. However, it can be argued that while the block size is insufficient to provide good statistics for an instantaneous area average, the size is sufficient to allow the controlling mechanism (Taylor wave instability) to be free of the boundary. For this situation, there will be instantaneous liquid contact 'small area' fraction, F_{SA}, measurements, which for a given surface superheat are the same as a true F_A. These F_{SA} will be the maximum F_{SA} the small area can measure for that surface superheat. Smaller values of F_{SA} are measured, but it is assumed that their frequency is much greater and that they could be time-averaged to still produce the maximum F_{SA} at this surface superheat. Yao and Henry also note that the contacts above the homogeneous nucleation temperature may not be actual contacts, but arise from local electrical discharges resulting from the high temperatures and their dc circuitry. For the current experiments, very limited contacts above the homogeneous nucleation temperature were observed (see Fig. 6). The detection of these high temperature contacts is very sensitive to the third criterion discussed in Appendix A. The above arguments offer an explanation, then, of why: (a) the current F_θ values lie near the upper bound of F_{SA} in Fig. 6; (b) there are many values of F_{SA} below the current data.

Also shown in Fig. 6 is the limited F_θ data of Nishikawa, [13] which only reports F_θ data for surface superheats up to 35 K, due to difficulty in reading their temperature traces above that superheat. The data are in reasonable agreement with the trends of the current data, considering the limited size of their boiling surface (8 mm diameter) relative to the most dangerous wavelength (2.7 cm). This small size assures that the 'jets and columns' phenomena will control their post-CHF boiling process as opposed to the Taylor instability. At these low surface superheats, however, it is not clear that the Taylor instability can continue to function [5]. Also, ref. [13]'s use of a thermocouple soldered into the boiling surface and exited up through the fluid should influence the nucleation process controlling the phenomena by creating additional artificial nucleation cavities at the measurement point. This effect should decrease the measured F_θ, but to what extent is unknown.

The frequency of liquid–solid contacts for the typical run (Run 1) is shown as a function of surface superheat in Fig. 7. The frequency of liquid–solid contact was <5 contacts/s with surface superheats >180 K. As the surface superheats decreased from 180 K, an increasingly unstable vapor film introduced a progressive breakdown of film boiling, resulting in a maximum liquid contact frequency of ~ 50 contacts/s

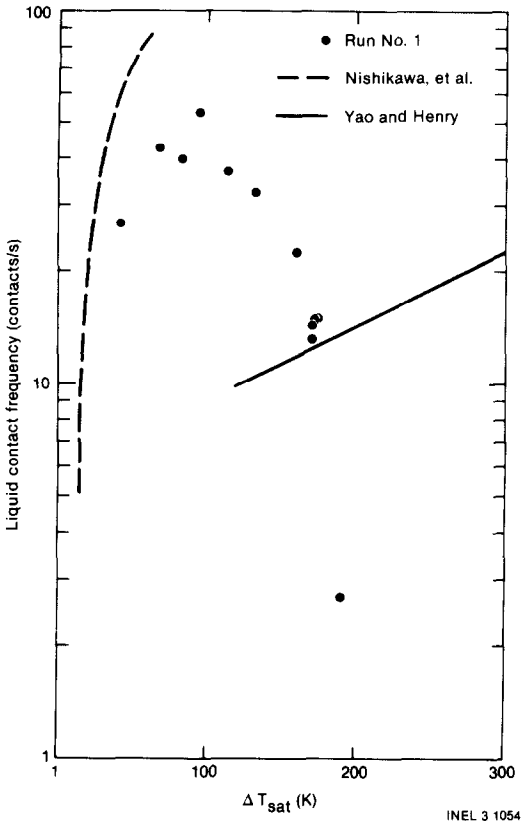

FIG. 7. Typical liquid–solid contact frequency vs wall superheat.

at 100 K superheat (a high contact frequency of 100 contacts s^{-1} was reported in Run Series I of [19]). As the wall superheat dropped below 100 K, a gradual drop in contact frequency to about 30 contacts s^{-1} occurred as critical heat flux was approached [19].

The frequency-of-contact results for Run 1 are also compared to other available frequency-of-contact data in Fig. 7. Typical data of Nishikawa [13] show frequencies higher than those of the present work for the superheat ranges available. However, the frequency increases as the surface superheat increases, which is the same trend of the current data over this low superheat range. In the case of the ref. [13] data, the artificial cavities created at the thermocouple-surface junction could increase the number of departing bubbles, and therefore increase the contact frequency. For completeness, the data of Yao and Henry [11] are also shown. Due to the 'small area' argument presented in the previous discussion of F_{SA}, the difference that exists should not be considered, since the frequency they measure is the contact frequency of their total area as opposed to the point contact frequency of the present work.

Figure 8 illustrates that the average duration of the liquid–solid contacts for Run 1 behaved much as expected, increasing with decreasing superheat. The average liquid–solid contact durations hovered around 1 ms with surface superheat > 80 K, and increased very rapidly to 15 ms before full liquid contact on the surface occurred.

Also shown on Fig. 8 are typical results from ref. [13], which have the same trends as the current data, but which are shorter in duration for a given wall superheat. As with the argument for F_θ and contact frequency, the difference created by the possibly different phenomena is unknown, but additional cavities creating more bubbles probably shorten the contact time. The measured contact times in the Yao and Henry results [12] can be seen in Fig. 6, but as with their frequency measurement, they reflect a quantity to which the current average contact duration should not be compared.

Figure 9 presents the liquid–solid contact duration distributions at various average surface superheats for Run 1. As expected, the distributions show that as the superheat decreases, the liquid–solid contact duration distribution shifts to include longer duration contacts. The shortest duration contact measured during these experiments was 0.5 ms, while the longest was generally < 32 ms before final quench. For Run 1 at an average surface superheat of 114.5 K [see Fig. 9(a)], ~37% of the liquid contacts that occurred were between 0.5 and 1.0 ms. Seventy-five percent of the contacts were < 2 ms, while 97% were < 4 ms. At low surface superheats [see Fig. 9(b)] the distribution is reversed from that of the high superheat. A typically flat distribution occurred at a surface superheat of ~80 K [see Fig. 9(c)].

Using the information in Fig. 9, an estimate of the maximum error produced by the microthermocouple response on F_θ can be obtained by considering the error in measured $\theta_{l,j}$ to be equal to the slowest measured

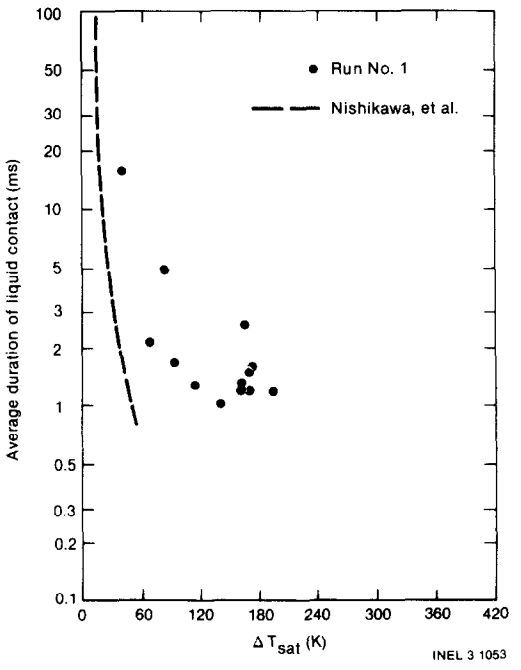

FIG. 8. Average duration of liquid–solid contact.

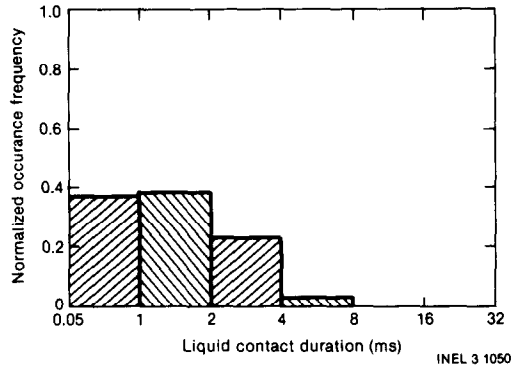

FIG. 9 (a). Liquid–solid contact duration distribution at surface superheat of 114.5 K for Run 1.

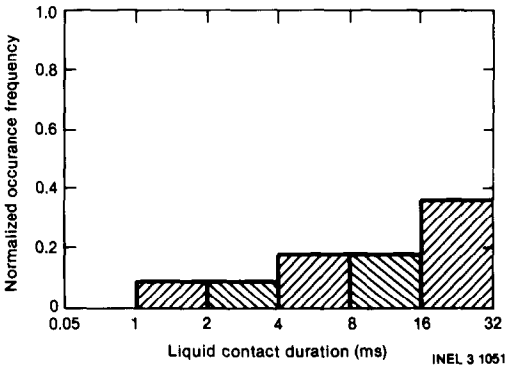

FIG. 9 (b). Liquid–solid contact duration distribution at surface superheat of 42.5 K for Run 1.

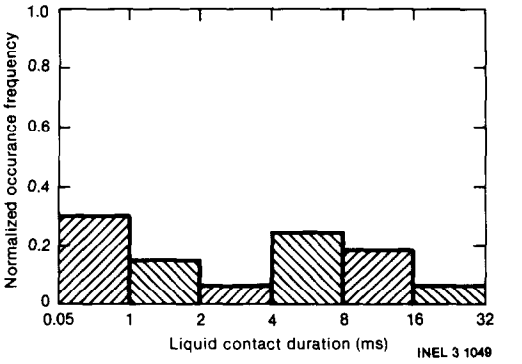

FIG. 9(c). Liquid–solid contact duration distribution at surface superheat of 84.8 K for run 1.

response time of 5 (10^{-5}) s. For the high surface superheat in Fig. 9(a), a maximum error for F_θ of 5% is calculated due to thermocouple response time. For the low surface superheat in Fig. 9(b), the error is $<1\%$. Therefore, combining this error with the maximum error due to the sampling window (discussed in ref. [18]), a maximum error for F_θ is obtained of $\sim 15\%$ for the high surface superheats ($90 \leqslant \Delta T_{sat} \leqslant 160$ K), 40% for the low surface superheats ($30 \leqslant \Delta T_{sat} \leqslant 60$ K), and hundreds of percent for the very high superheats ($\Delta T_{sat} > 180$ K).

LOCAL SURFACE TEMPERATURE

The above results describing characteristics of liquid–solid contacts have been presented in reference to the surface superheat (Figs. 5–8). For these results, the surface superheats were measured by the same microthermocouple probe. At a much slower sampling frequency (20 s^{-1}) than that used in obtaining liquid contact information, it is possible to record the overall surface temperature history throughout the quench process. As shown in Fig. 2, a typical quench history passes from stable film boiling, through transition boiling, and into the nucleate boiling regime. In most boiling experiments, all temperatures are normally measured by thermocouples imbedded in the wall at some depth below the boiling surface. Such imbedded thermocouples have slow response times and are insensitive to the short-term phenomena associated with individual bubbles or liquid contacts on the boiling surface. Inverse conduction calculations from these measured temperatures are normally utilized to infer time-averaged wall surface temperatures. With the surface thermocouple used in this investigation, a more direct measurement of the surface temperature is obtained. However, because of its small localized sensing junction and fast response, this probe provides a measurement of the transient surface temperature that is sensitive to individual liquid contacts or bubble phenomena. Therefore, to obtain a comparable time-averaged surface temperature, it was necessary to integrate the surface thermocouple signal over a finite window of time. The procedure used was to average the probe signal over windows of 0.8 s. These time-averaged temperatures were then utilized to determine the wall surface superheat, ΔT_{sat}, shown in Figs. 5–8.

Once the time-averaged surface superheat was obtained, it was also possible to determine the transient surface heat flux by one-dimensional, inverse-conduction analysis. Following the method of Beck [20], such analyses have been performed and the resulting boiling curves are given in ref. [19]. Calculations of the heat flux were made [19], using the simple concept originally proposed by Bankoff and Mehra [10], and compared to the reduced boiling curves. Neglecting the vapor contribution and using measured contact data, two limiting cases for the heat flux were calculated using the solution [21] for two semi-infinite media at different temperatures brought together. The lower limit used the $k\rho c$ of water and represented the conduction transport limit imposed by the liquid. Under normal situations, internal circulation and turbulence within the liquid will increase the effective thermal conductivity of the contacting liquid. An upper limit exists when the effective thermal conductivity of the liquid becomes so high that the heat transfer rate is limited by the base metal, i.e. the $k\rho c$ of the liquid tends towards infinity. These limiting cases were found to bound the reduced boiling curves indicating that liquid–solid contacts may be the

dominant mechanism for energy transfer in the transition boiling process.

CONCLUSIONS

A special microthermocouple surface probe was successfully employed to obtain direct measurements of liquid–solid contacts in film and transition boiling of water at atmospheric pressure. The local liquid contact-time fraction, F_θ, decreased from ~ 0.5 at a surface superheat of 30 K to ~ 0.003 at a surface superheat of 200 K. The frequency of occurrence of liquid contact was found to have a maximum value of ~ 50 contacts s^{-1}, at surface superheat of ~ 100 K. The average duration of liquid contact decreased steeply with increasing surface superheat, varying from ~ 15 ms at 30 K superheat to ~ 1 ms at 120 K superheat. The frequency distribution for liquid contacts shows that short duration contacts dominate at high wall superheat and relatively long liquid contacts dominate at low wall superheats. While these boiling-curve results are not presented explicitly in this paper, the results indicate that liquid–solid contacts may be the dominant mechanism for energy transfer in the transition pool boiling process. It is hoped that both the instrument and the technique discussed will prove useful in future investigations to further the understanding of liquid–solid contact phenomena.

REFERENCES

1. R. H. Winterton, Transition boiling, Atomic Energy Establishment Winfrith Report AEEW-R 1567 (1982).
2. D. C. Groeneveld and C. W. Snock, A review of current heat transfer correlations used in reactor safety assessments, Proceedings of Second International Topical Meeting on Nuclear Reactor Thermal-Hydraulics 0-28 (1983).
3. D. C. Groeneveld and C. W. Snock, A comprehensive examination of heat transfer correlations suitable for reactor safety analysis, Atomic Energy of Canada Limited Report AECL-7838 (1982).
4. W. M. Rohsenow, *Heat Transfer—A Symposium*. University of Michigan, Ann Arbor (1952).
5. L. C. Witte and J. H. Lienhard, On the existence of two 'transition' boiling curves, *Int. J. Heat Mass Transfer* **25**, 771–779 (1982).
6. J. W. Westwater and J. G. Santangelo, Photographic study of boiling, *I&EC Fundamentals* **47**, 1605–1610 (1955).
7. B. J. Stock, Observations on transition boiling heat transfer phenomena, ANL 6175 (1960).
8. P. J. Berenson, Experiments on pool boiling heat transfer, *Int. J. Heat Mass Transfer* **5**, 985–999 (1962).
9. W. S. Bradfield, Liquid–solid contacts in stable film boiling, *I&EC Fundamentals* **5**, 200–204 (1966).
10. S. G. Bankoff and V. S. Mehra, A quenching theory for transition boiling, *I&EC Fundamentals* **1**, 38–40 (1962).
11. S. C. Yao and R. E. Henry, Hydrodynamic instability induced liquid–solid contacts in film boiling, ASME Winter Annual Meeting 76-WA/HT-25 (1976).
12. S. C. Yao and R. E. Henry, An investigation of the minimum film boiling temperature on horizontal surfaces, *J. Heat Transfer* **100**, 260–267 (1978).
13. K. Nishikawa, T. Fujii, and A. Honda, Experimental study on the mechanism of transition boiling heat transfer, *Bull ASME*, **15**, 93–103 (1972).
14. L. Y. W. Lee, J. C. Chen, and R. A. Nelson, A surface probe for measurement of liquid contact in film and transition boiling on high temperature surfaces, *Rev scient. Instrum.* **53**, 1472–1476 (1982).
15. O. C. Iloeje, D. N. Plummer, W. M. Rohsenow, and P. Griffith, An investigation of the collapse and surface rewet in film boiling in forced vertical flow, *J. Heat Transfer* **97** 166–172 (1975).
16. J. C. Chen, R. K. Sundaram, and F. T. Ozkaynak, A phenomenological correlation for post-CHF heat transfer, Lehigh University Department of Mechanical Engineering Report TS-774 (1977).
17. H. S. Ragheb and S. C. Cheng, Surface wetted area during transition boiling in forced convective flow, *J. Heat Transfer* **101**, 381–383 (1979).
18. L. Y. W. Lee, J. C. Chen, and R. A. Nelson, Liquid–solid contact measurements using a surface thermocouple temperature probe in atmospheric pool boiling water, to be presented at the 1984 Heat Transfer Conference, Niagara Falls, N.Y., (1984).
19. L. Y. W. Lee, Measurements of liquid contact in pool boiling of water using a fast response surface temperature probe method, M.S. thesis, Lehigh University (1982).
20. J. V. Beck, Review of six inverse heat conduction computer codes, ANL Report (1981).

MESURE DE CONTACT LIQUIDE–SOLIDE UTILISANT UNE SONDE DE TEMPERATURE DE SURFACE A THERMOCOUPLE DANS L'EAU BOUILLANT A PRESSION ATMOSPHERIQUE EN RESERVOIR

Résumé—L'objet de cette étude est d'appliquer la technique utilisant un microthermocouple à la surface d'ébullition pour la mesure de l'histoire de la température de surface locale pendant l'ébullition en film et en transition. De ces mesures sont observés des contacts directs liquide–solide dans ces régimes d'ébullition. En ébullition d'eau saturée, distillée et déionisée sur une surface de cuivre recouverte d'aluminium, la fraction de temps de contact local avec le liquide augmente quand la surchauffe de la surface diminue. La durée moyenne de contact croît de façon monotone quand la surchauffe de la surface décroît, tandis que la fréquence de contact liquide atteint un maximum proche de 50 contacts/s pour une surchauffe de 100 K environ et elle décroît graduellement jusqu'à 30 contacts/s près du flux critique. La distribution de temps de contact liquide–solide est dominée par des contacts brefs inférieurs à 4 ms pour les fortes surchauffes et elle atteint des contacts prolongés supérieurs à 4 ms pour les faibles surchauffes, en passant par une distribution assez plate de durée de contact vers 80 K. Les résultats de cet article montrent que les contacts liquide–solide peuvent être le mécanisme dominant du transfert d'énergie dans le mécanisme d'ébullition de transition.

FLÜSSIG–FEST-KONTAKTZEIT-MESSUNGEN MITTELS EINES OBERFLÄCHEN-THERMOELEMENTS BEIM BEHÄLTERSIEDEN VON WASSER BEI ATMOSPHÄRENDRUCK

Zusammenfassung—In dieser Untersuchung wurde ein in die Siedeoberfläche eingelassenes Mikro-Thermoelement zur Messung der zeitlichen Veränderung der lokalen Oberflächentemperaturen beim Film- und Übergangssieden an Hochtemperaturoberflächen verwendet. Aufgrund dieser Messungen konnte der direkte Kontakt zwischen Flüssigkeit und Feststoff beim Film- und Übergangssieden verfolgt werden. Beim Behältersieden von gesättigtem, destilliertem, deionisiertem Wasser an einer aluminiumbeschichteten Kupferoberfläche steigt der zeitgemittelte lokale Flüssigkeitskontaktanteil mit fallender Wandübertemperatur. Die mittlere Kontaktzeit steigt monoton mit sinkender Übertemperatur der Oberfläche, während die Frequenz des Flüssigkeitskontakts bei ~ 100 K Wandübertemperatur ein Maximum von ~ 50 Kontakten/s erreicht und langsam auf 30 Kontakte/s in der Nähe der kritischen Wärmestromdichte absinkt. Die Verteilung der Kontaktzeit zwischen Flüssigkeit und Feststoff wurde bei großen Wandüberhitzungen durch kurze Kontaktzeiten < 4 ms bestimmt und verschob sich zu langen Kontaktzeiten > 4 ms bei kleinen Wandüberhitzungen, wobei eine relativ flache Kontaktzeitverteilung bei etwa 80 K Wandübertemperatur durchlaufen wurde. Die Ergebnisse dieser Arbeit deuten an, daß die Kontakte zwischen Flüssigkeit und Feststoff ein bestimmender Mechanismus des Energietransports beim Übergangssieden sein könnten.

ИЗМЕРЕНИЯ НА ГРАНИЦЕ ЖИДКОСТЬ-ТВЕРДОЕ ТЕЛО С ИСПОЛЬЗОВАНИЕМ ПОВЕРХНОСТНОГО ТЕМПЕРАТУРНОГО ДАТЧИКА С ТЕРМОПАРОЙ ПРИ КИПЕНИИ ВОДЫ В БОЛЬШОМ ОБЪЕМЕ В АТМОСФЕРНЫХ УСЛОВИЯХ

Аннотация—Для измерения изменения во времени местной температуры поверхности при пленочном нестационарном кипении на высокотемпературных поверхностях используются микротермопары, вмонтированные заподлицо с поверхностью кипения. В результате измерений получены данные по прямому контактированию жидкости и твердого тела в режимах пленочного и нестационарного кипения. При кипении большого объема насыщенной, дистиллированной, деионизованной воды на покрытой алюминием медной поверхности показатель, характеризующий осредненную по времени составляющую локального контакта жидкости с поверхностью, растет с уменьшением перегрева поверхности. Осредненная продолжительность контакта возрастает монотонно с уменьшением перегрева поверхности, в то время как частота контакта с жидкостью достигает максимума (~ 50 контактов/с) при перегреве поверхности (~ 100 К), и постепенно убывает до 30 контактов в секунду при критическом тепловом потоке. Для большого перегрева поверхности распределение продолжительности контакта жидкость-твердое тело в основном определяется короткими контактами < 4 мс и смещается в сторону более длительных контактов > 4 мс при низких перегревах поверхности, проходя через относительно ровное распределение продолжительности контакта при температуре ~ 80 К. Результаты работы показывают, что контакты жидкость–твердое тело в процессах нестационарного кипения могут быть преобладающим механизмом энергообмена.